Coulomb Drag at Zero Temperature

Alex Levchenko and Alex Kamenev

Department of Physics, University of Minnesota, Minneapolis, Minnesota 55455, USA

(Received 11 October 2007; published 16 January 2008)

We show that the Coulomb drag effect exhibits saturation at small temperatures, when calculated to the third order in the interlayer interactions. The zero-temperature transresistance is of the order $h/(e^2g^3)$, where g is the dimensionless sheet conductance. The effect is therefore the strongest in low mobility samples. This behavior should be contrasted with the conventional (second order) prediction that the transresistance scales as a certain power of temperature and is (almost) mobility independent. The result demonstrates that the zero-temperature drag is not an unambiguous signature of a strongly coupled state in double-layer systems.

DOI: 10.1103/PhysRevLett.100.026805 PACS numbers: 73.23.−b, 73.50.−h, 73.61.−r

The Coulomb drag effect has proven to be a sensitive probe of electron-electron (e-e) interactions. The phenomenon is usually observed [1–6] in double-layer systems, where electrons interact through the long-ranged Coulomb forces. A current, passing through one of the layers (the active layer), induces a voltage across the second (passive) layer. The ratio between the two, the so-called drag *transresistance* ρ_D, carries valuable information about the state of electrons in each of the layers, as well as the nature of their mutual interactions.

The transresistance for weakly interacting electrons was calculated [7–11] in the second order in the screened interlayer interaction and found to be given by

$$\rho_D(T) = 0.12\frac{h}{e^2}\left(\frac{T}{E_F}\right)^2\frac{1}{(\kappa d)^2(k_F d)^2}, \qquad (1)$$

where d is the separation between the layers, E_F and k_F are the Fermi energy and momentum correspondingly, and κ is the inverse Thomas-Fermi screening radius. This result is in reasonable agreement with a number of experiments [1–4]. Its main feature is the quadratic temperature dependence, which may be traced back to the phase volume accessible for the interlayer e-e scattering. The second order effect requires electron-hole asymmetry, i.e., the difference in velocity between electrons and holes on the opposite sides of the Fermi surface. Such an asymmetry scales as E_F^{-1} for each of the two layers, giving rise to the factor E_F^{-2} in Eq. (1). The latter serves as the dimensional scale, which normalizes the T^2 dependence.

On the other hand, the systems with strong interlayer correlations are predicted to exhibit a *nonzero* drag transresistance ($\propto h/e^2$) even at *zero temperature*. The examples include 1D charge density waves at exact commensurability [12], as well as Quantum Hall bilayer structures at the total filling factor $\nu = 1$ [13]. In the latter system the effect was likely observed experimentally in Ref. [14]. This raises a question if $\rho_D(0)$ may serve as an unambiguous indicator of a strongly correlated state in a system at hand, i.e., whether the drag transresistance undergoes a quantum phase transition between the weakly-coupled state, where it is strictly zero, and a strongly-coupled phase, where it is finite.

In this Letter we give a strong argument against such a scenario. We show that $\rho_D(0) \neq 0$ already in *weakly interacting* bilayer systems. To this end we evaluate the transresistance in the *third* order in the (screened) interlayer interactions and find a constant temperature-independent contribution

$$\rho_D(T) = 0.27\frac{h}{e^2}\frac{1}{g^3}\frac{1}{(\kappa d)^2}; \qquad T < h/\tau, \qquad (2)$$

where $g = 25.8k\Omega/\rho_\square$ is the dimensionless conductance (here $\rho_\square$ is the resistance of the single layer) and τ is the elastic scattering time. Drag effect, saturating at small temperatures, is therefore *not* an automatic indicator of a strongly correlated state.

There are general reasons to expect that the third-order effect may be qualitatively different from the second order one, Eq. (1). Indeed, the third-order transresistance does *not* rely on the electron-hole asymmetry. This is because the corresponding linear-response diagrams involve *four*-leg vertices (see below) which do not vanish within linearized dispersion relation approximation (i.e., in the electron-hole symmetric case). Therefore, the result is expected to be independent of the Fermi energy, E_F. Since we are interested in the lowest temperatures, it is natural to focus on the diffusive regime, where $T \ll h/\tau$. In this regime there is no other relevant energy, which may provide a scale for a temperature dependence. Hence, the temperature-independent result, Eq. (2), is not entirely unexpected. Moreover, the four-leg vertex, mentioned above, is known to play a central role in the low-temperature transport of diffusive metals. It is exactly this object that gives rise to singular Altshuler-Aronov (AA) corrections to the intralayer conductance [15].

Coming from another perspective, it is certainly unusual to find a temperature-independent result for the quantity which relies on the e-e scattering rate. Indeed, the latter is

proportional to the available phase volume around the Fermi surface, which scales as T^2. However, in addition to the occupation numbers the scattering rate is proportional to a certain matrix element (the overlap integral of six wave functions for the third-order process, considered here). In diffusive systems such matrix elements are known to be singularly enhanced in the limit where all involved states are close in energy [16]. It is exactly this enhancement that leads to singular *e-e* interaction effects in the low-temperature diffusive limit [17]. In the case of the third-order transconductance in 2D the smallness of the phase volume is exactly compensated by the divergence of the corresponding matrix elements. This yields the temperature-independent transresistance, Eq. (2). The diffusive enhancement of the matrix elements is less pronounced in cleaner systems. Hence, in the clean limit, $g \to \infty$, the zero-temperature drag, Eq. (2), disappears.

There are two limitations on the applicability of Eq. (2) at very low temperatures. (i) Once the temperature length $L_T = \sqrt{hD/T}$, where D is the diffusion constant, reaches the sample size L, the growth of the matrix elements is saturated. As a result, $\rho_D \propto T^2$ at $T < E_{\mathrm{Th}}$, where $E_{\mathrm{Th}} = hD/L^2$ is the Thouless energy. (ii) If the sample size is very big, one may enter the regime of disorder and/or interaction induced localization. The relevant temperature scale is that where the AA correction $\sigma_\square = e^2/h[g - \pi^{-1}\ln(h/T\tau)]$ [15] is significant, i.e., $T \sim (h/\tau)e^{-\pi g}$. At smaller temperatures the diffusive approximation breaks down and our result, Eq. (2), is not applicable.

A natural question is why in the experiments of, e.g., Refs. [1–3] the low-temperature saturation of $\rho_D(T)$ was not observed. In order to answer, one may estimate the saturation temperature T^* by equating Eqs. (1) and (2). This way, one finds $T^* \approx E_F(k_F d)g^{-3/2}$. Employing the parameters of, e.g., Ref. [2]: $E_F \approx 60$ K, $g \approx 100$, and $k_F d \approx 4$, one finds $T^* \approx 0.25$ K and the residual resistance $\rho_D \approx 0.4$ mΩ as it follows from the Eq. (2). At the same time the lowest temperature reported in Ref. [2] $T \approx 0.5$ K and the corresponding drag $\rho_D \approx 0.65$ mΩ are just above the expected saturation. The similar situation is true regarding most of the other reports of the Coulomb drag [1,3–5].

It is rather likely, though, that the saturation observed by Lilly *et al.* [18] in $\nu = 1$ Quantum Hall bilayer system in the composite fermion regime is a manifestation of Eq. (2). Indeed, it was shown [19] that the diffusive corrections in the composite fermion regime are rather similar to those in zero magnetic field. Virtually the only difference is a substantial downward renormalization of the composite fermion conductance g^{cf}, as compared to that in the zero field, g. Estimating $g^{\mathrm{cf}} \approx 10$ and $E_F^{\mathrm{cf}} \approx 5$ K for the samples of Ref. [18], one finds $T^* \approx 0.15$ K and $\rho_D(0) \approx 2\ \Omega$ in good agreement with Ref. [18]. To verify Eq. (2), more experiments in zero magnetic field with smaller g or/and smaller temperatures are needed.

The four-leg vertex, which is a building block for diagrams of the third-order drag transconductance is depicted in Fig. 1. It describes an induced nonlinear interaction of electromagnetic fields through excitation of electron-hole pairs in a given layer. The vertex is nonlocal because of the diffusive propagation of the electron-hole excitations within the layer. The latter is encoded in the propagator

$$\mathcal{D}_\alpha(q,\omega) = \frac{1}{\nu_\alpha}\frac{1}{D_\alpha q^2 - i\omega}, \tag{3}$$

where ν_α is the density of states of the layer $\alpha = 1, 2$ and D_α is its diffusion coefficient. Notice that the dimensionless conductance is expressed as $g_\alpha = \nu_\alpha D_\alpha$.

We work with the Keldysh technique [20–22]. In its framework the fluctuating electromagnetic potentials acquire an additional index: classical (cl) or quantum (q), which stay for symmetric and antisymmetric combinations of the fields propagating forward and backward in time, correspondingly. The proper indices are indicated in Fig. 1. The fact that the four-leg vertex of this very structure is unique in the leading order in $1/g_\alpha$ may be rigorously proven within Keldysh nonlinear sigma-model [21]. In fact, it is exactly this vertex which gives rise to the singular AA correction [15]. The latter is obtained by pairing one classical and one quantum electromagnetic potentials, while the two remaining ones represent an external (classical) electric field along with induced current [21].

It is convenient to work in a gauge, where the Coulomb interactions are mediated by the longitudinal vector potentials, rather than the scalar potentials. An advantage of using such a gauge is that both internal and external potentials, as well as the current sources, are all expressed through the same type of field. This makes the structure of the vertex, Fig. 1, particularly symmetric. Moreover, the gauge may be chosen in a way that the propagator of the longitudinal vector potentials $\mathcal{V}_{\alpha\beta} = 2i\langle A^{cl}_\alpha A^q_\beta\rangle$ automatically includes the vertex renormalization by the disorder [21]

$$\mathcal{V}_{\alpha\beta}(q,\omega) = \frac{q^2 V^R_{\alpha\beta}(q,\omega)}{(D_\alpha q^2 - i\omega)(D_\beta q^2 - i\omega)}, \tag{4}$$

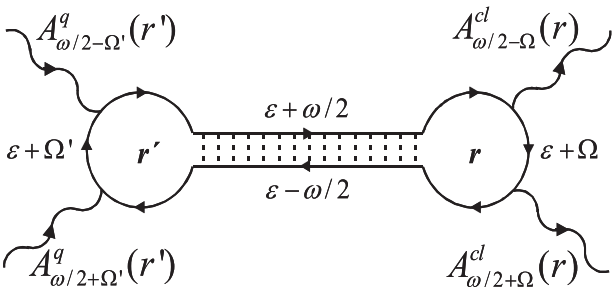

FIG. 1. The four-leg vertex, central to the third-order drag effect, as well as to the intralayer AA correction. External wavy lines represent fluctuating vector potentials; the ladder is the diffusion propagator $\mathcal{D}(r - r', \omega)$.

where $V^R_{\alpha\beta}(q,\omega)$ is the 2×2 matrix of retarded intralayer and interlayer interactions calculated within random phase approximation (RPA). The latter is the solution of the standard Dyson equation [10,11] $\hat{V}^R = \hat{V}_0 + \hat{V}_0\hat{\Pi}\hat{V}^R$, where

$$\hat{V}_0 = \frac{2\pi e^2}{q}\begin{pmatrix} 1 & e^{-qd} \\ e^{-qd} & 1 \end{pmatrix}, \qquad \hat{\Pi} = \begin{pmatrix} \frac{\nu_1 D_1 q^2}{D_1 q^2 - i\omega} & 0 \\ 0 & \frac{\nu_2 D_2 q^2}{D_2 q^2 - i\omega} \end{pmatrix}. \tag{5}$$

Note that the polarization operator $\hat{\Pi}(q,\omega)$ has no off-diagonal elements, reflecting the absence of tunneling between the layers.

We are now in a position to evaluate the third-order drag transconductance. The corresponding diagrams are constructed from the two vertices of Fig. 1; one for each of the layers is shown in Fig. 2. Remarkably, there are only two ways to connect them, using the propagators (4) (recall that $\langle A^q_\alpha A^q_\beta\rangle = 0$ [22]). The analytic expression for the sum of the two diagrams of Fig. 2 is given by

$$\sigma_D = 32e^2 T g_1^2 g_2^2 \int_0^\infty \frac{d\omega d\Omega}{4\pi^2}\mathcal{F}_1\mathcal{F}_2 \sum_{q,Q} \mathrm{Im}\Big[\mathcal{D}_1(q,\omega)\mathcal{D}_2(q,\omega)\mathcal{V}_{12}(q,\omega)\mathcal{V}_{12}\Big(\frac{q}{2}-Q,\frac{\omega}{2}-\Omega\Big)\mathcal{V}_{12}\Big(\frac{q}{2}+Q,\frac{\omega}{2}+\Omega\Big)\Big]. \tag{6}$$

The two functions $\mathcal{F}_1(\omega,\Omega)$ and $\mathcal{F}_2(\omega,\Omega)$ originate from the integration over the fast electronic energy ε (see Fig. 1), in the active and passive layers correspondingly. In the dc limit they are given by

$$\mathcal{F}_1(\omega,\Omega) = T\frac{\partial}{\partial\Omega}[\mathcal{B}(\Omega+\omega/2) - \mathcal{B}(\Omega-\omega/2)], \tag{7a}$$

$$\mathcal{F}_2(\omega,\Omega) = 2 - \mathcal{B}(\Omega+\omega/2) - \mathcal{B}(\Omega-\omega/2) + \mathcal{B}(\omega), \tag{7b}$$

$$\mathcal{B}(\omega) = \frac{\omega}{T}\coth\Big(\frac{\omega}{2T}\Big). \tag{7c}$$

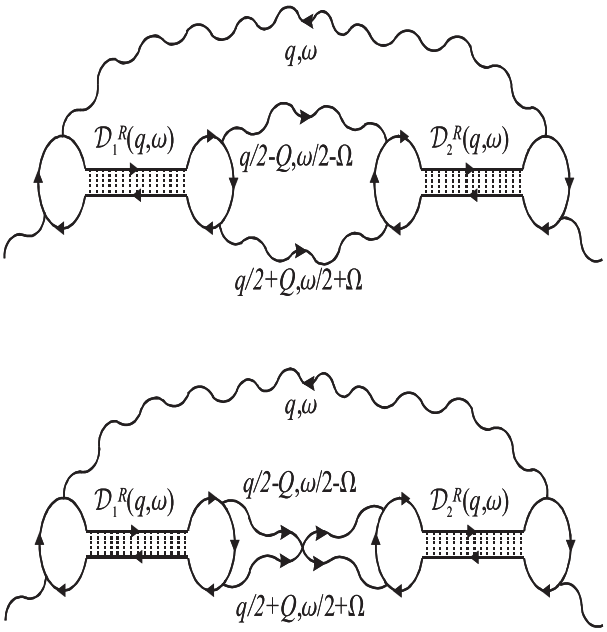

FIG. 2. Two diagrams for the drag transconductance σ_D in the third order in the interlayer interactions, $\mathcal{V}_{12}(q,\omega)$, denoted by wavy lines. The intralayer diffusion propagators $\mathcal{D}_\alpha(q,\omega)$, Eq. (3), are denoted by ladders.

To make the further calculations more compact, we restrict ourselves to the identical layers. We first consider the experimentally most relevant case of the long-ranged coupling, where $\kappa d \gg 1$. Here $\kappa = 2\pi e^2\nu$ is the Thomas-Fermi inverse screening radius. In this limit the effective interlayer interaction potential, Eqs. (4) and (5), acquires a simple form

$$\mathcal{V}_{12}(q,\omega) = \frac{1}{g}\frac{1}{\kappa d D q^2 - 2i\omega}. \tag{8}$$

Next, we substitute Eqs. (3), (7), and (8) into Eq. (6) and perform the energy and momentum integrations. The inspection of the integrals shows that both energies ω and Ω are of the order of the temperature $\omega \sim \Omega \sim T$ (in compliance with the phase volume considerations) [23]. On the other hand, the characteristic value of the transferred momenta is $q \sim Q \sim \sqrt{T/(D\kappa d)} \ll \sqrt{T/D}$ [cf. Equation (8)]. Therefore one may disregard Dq^2 as compared to $i\omega$ in the expressions for $\mathcal{D}_\alpha(q,\omega)$, Eq. (3), approximating the product $\mathcal{D}_1\mathcal{D}_2$ in Eq. (6) by $-\omega^{-2}$. This factor represents the diffusive enhancement of the matrix elements, mentioned in the introduction. Such spatial scales separation implies that the four-leg vertices, Fig. 1, are effectively spatially local, while the three interlayer interaction lines are long-ranged.

Rescaling energies by T and momenta by $\sqrt{T/(D\kappa d)}$, one may reduce the expression (6) for the transconductance to $\sigma_D = (e^2/h)g^{-1}(\kappa d)^{-2} \times$ (dimensionless integral). The latter integral does not contain any parameters and is free from divergences in all directions. It is thus simply a number that may be evaluated numerically [24]. In the limit $\sigma_D \ll (e^2/h)g_\alpha$ the transresistance is related to σ_D by $\rho_D = \sigma_D h^2/(e^4 g_1 g_2)$, resulting finally in Eq. (2).

To emphasize the fact that the scale separation, discussed above, is *not* crucial for having the low-temperature saturation, we briefly consider the case of the short-ranged interlayer interactions, $V^R_{12}(q,\omega) = V_0$. The latter may be relevant, if interactions are screened by, e.g., metallic back gate. One employs then Eqs. (3) and (4) and rescales the

energies by the temperature and the momenta by $\sqrt{T/D}$. This way the transconductance, Eq. (6), once again reduces to the dimensionless and parameter free integral. The latter is convergent in all directions and may be readily evaluated, resulting in

$$\rho_D = 0.01 \frac{h}{e^2} \frac{1}{g^3} (\nu V_0)^3. \quad (9)$$

Notice that the effect is expected to have the negative sign for the short-ranged *attractive* interactions. This observation may have relevance for oppositely doped double-layer structures.

The low-temperature saturation of the Coulomb drag was discussed previously in Refs. [25,26]. Both of them considered essentially different and somewhat more exotic mechanisms. The zero-temperature saturation suggested in Ref. [25] relies on the assumption that the electrons in both layers are scattered by exactly the same disorder potential. Ref. [26] focuses on the strongly coupled regime, where the pairing order parameter is suppressed by disorder.

To conclude, we have studied the Coulomb drag phenomenon in weakly interacting bilayer systems and have found that the effect saturates at small temperatures, when calculated to the third order in the interlayer interactions. The saturation of drag relies on the presence of disorder and scales inversely with mobility. It does not require, though, any correlations of the disorder potential in the two layers. The effect was possibly observed in Ref. [18], although more experiments in lower mobility samples and zero magnetic field are highly desirable.

We are grateful to D. Bagrets, L. Glazman, I. Gornyi, F. von Oppen, A. Savchenko, B. Shklovskii, and A. Stern for stimulating discussions. This work was supported by NSF Grant No. DMR 0405212. A. K. is also supported by the A. P. Sloan foundation.

[1] P. M. Solomon, P. J. Price, D. J. Frank, and D. C. La Tulipe, Phys. Rev. Lett. **63**, 2508 (1989).
[2] T. J. Gramila, J. P. Eisenstein, A. H. MacDonald, L. N. Pfeiffer, and K. W. West, Phys. Rev. Lett. **66**, 1216 (1991).
[3] U. Sivan, P. M. Solomon, and H. Shtrikman, Phys. Rev. Lett. **68**, 1196 (1992).
[4] M. Kellogg, J. P. Eisenstein, L. N. Pfeiffer, and K. W. West, Solid State Commun. **123**, 515 (2002).
[5] A. S. Price, A. K. Savchenko, B. N. Narozhny, G. Allison, and D. A. Ritchie, Science **316**, 99 (2007).
[6] R. Pillarisetty, H. Noh, D. C. Tsui, E. P. De Poortere, E. Tutuc, and M. Shayegan, Phys. Rev. Lett. **89**, 016805 (2002).
[7] B. Laikhtman and P. M. Solomon, Phys. Rev. B **41**, 9921 (1990).
[8] A.-P. Jauho and H. Smith, Phys. Rev. B **47**, 4420 (1993).
[9] L. Zheng and A. H. MacDonald, Phys. Rev. B **48**, 8203 (1993).
[10] A. Kamenev and Y. Oreg, Phys. Rev. B **52**, 7516 (1995).
[11] K. Flensberg, B. Y.-K. Hu, A.-P. Jauho, and J. M. Kinaret, Phys. Rev. B **52**, 14761 (1995).
[12] Y. V. Nazarov and D. V. Averin, Phys. Rev. Lett. **81**, 653 (1998).
[13] A. Stern and B. I. Halperin, Phys. Rev. Lett. **88**, 106801 (2002).
[14] M. Kellogg, J. P. Eisenstein, L. N. Pfeiffer, and K. W. West, Phys. Rev. Lett. **90**, 246801 (2003).
[15] B. L. Altshuler and A. G. Aronov, Zh. Eksp. Teor. Fiz. **77**, 2028 (1979) [Sov. Phys. JETP **50**, 968 (1979)].
[16] Ya. M. Blanter and A. D. Mirlin, Phys. Rev. E **55**, 6514 (1997); B. L. Altshuler, Y. Gefen, A. Kamenev, and L. S. Levitov, Phys. Rev. Lett. **78**, 2803 (1997).
[17] B. L. Altshuler and A. G. Aronov, in *Electron-Electron Interactions in Disordered Systems*, edited by A. J. Efros and M. Pollak (Elsevier, Amsterdam, 1985).
[18] M. P. Lilly, J. P. Eisenstein, L. N. Pfeiffer, and K. W. West, Phys. Rev. Lett. **80**, 1714 (1998).
[19] D. V. Khveshchenko, Phys. Rev. Lett. **77**, 362 (1996); A. D. Mirlin and P. Wolfle, Phys. Rev. Lett. **78**, 3717 (1997).
[20] L. V. Keldysh, Zh. Eksp. Teor. Fiz. **47**, 1515 (1964) [Sov. Phys. JETP **20**, 1018 (1965)].
[21] A. Kamenev and A. Andreev, Phys. Rev. B **60**, 2218 (1999).
[22] A. Kamenev, in *Nanophysics: Coherence and Transport*, edited by H. Bouchiat *et al.* (Elsevier, New York, 2005), p. 177.
[23] This behavior should be contrasted with the AA effect [15,17], where the frequency integral comes from the range $T \lesssim \omega \lesssim h/\tau$.
[24] The evaluation of the integrals over momenta is substantially simplified by the local nature of the vertex (in the limit $\kappa d \gg 1$). Transforming to the real space representation, the fourfold momentum integral in Eq. (6) reduces to

$$\int_0^\infty dr r \mathrm{Im}[K_0(r\mu)K_0(r\mu_+)K_0(r\mu_-)] = M(x, y),$$

where $K_0(r\mu)$ is the modified Bessel function, which is the 2D Fourier transform of the interaction potential (8). Here $\mu = \sqrt{-ix}$ and $\mu_\pm = \sqrt{-i(\pm y + x/2)}$, the radius is normalized by $\sqrt{D\kappa d/(2T)}$, and $x = \omega/T$; $y = \Omega/T$. Finally, the number of interest is given by

$$-2\pi^{-3} \iint_0^\infty dx dy \mathcal{F}_1(x, y)\mathcal{F}_2(x, y)x^{-2}M(x, y) \approx 0.27.$$

[25] I. V. Gornyi, A. G. Yashenkin, and D. V. Khveshchenko, Phys. Rev. Lett. **83**, 152 (1999).
[26] F. Zhou and Y. B. Kim, Phys. Rev. B **59**, R7825 (1999).